Figure S1 Hayashi. *et al*.

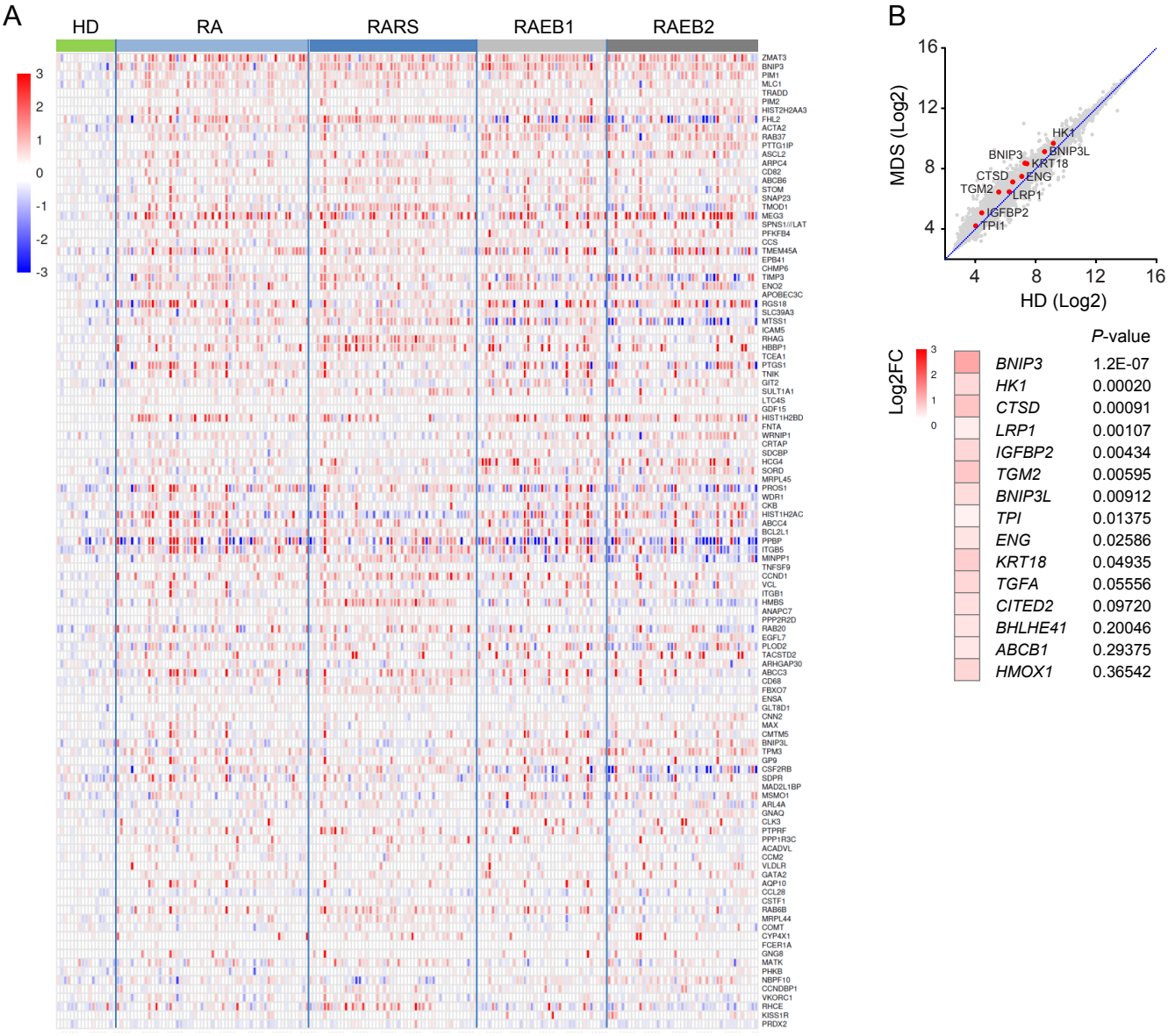

Figure S1. Activated HIF1A-associated Gene Expression in Human MDS. A, The leading edge genes from the gene set enrichment analysis of HIF1A induced genes in Figure 1A. **B,** Scatter plots comparing log2 expression of individual genes in CD34^{+} BM cells from MDS patients (n = 183) relative to healthy donor (n = 17). Known HIF1A target genes(1) upregulated in MDS patients are shown with red dots ($P < 0.05$).

Figure S2 Hayashi. *et al*.

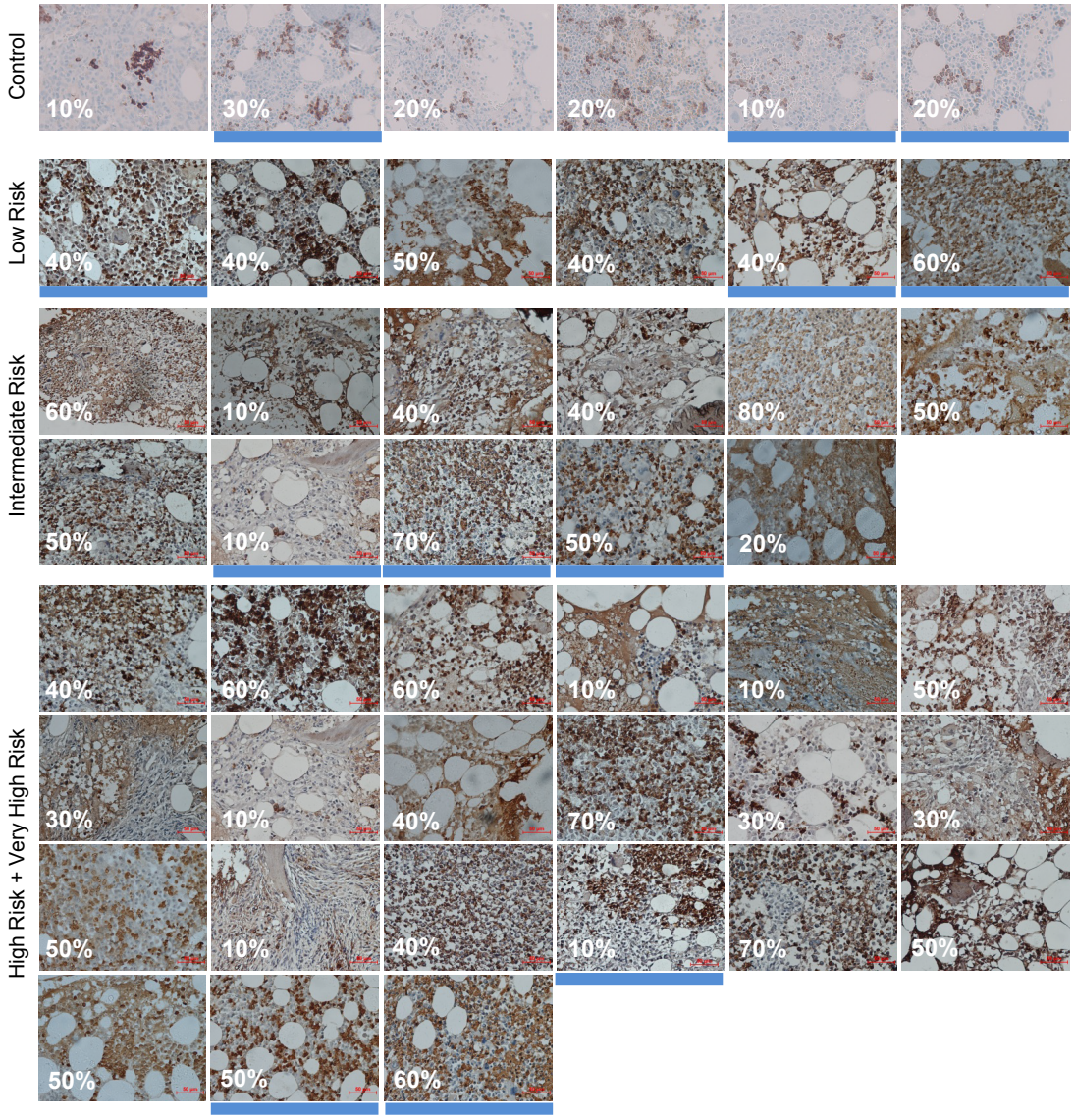

Figure S2. HIF1A Expression in the BM from Human MDS. HIF1A immunohistochemistry staining of MDS BM biopsy samples and de-identified adult BM samples diagnosed as apparently normal. Percentage indicates the frequency of HIF1A expressing cells. Underlined cases are shown in Figure 1B.

Figure S3 Hayashi. *et al*.

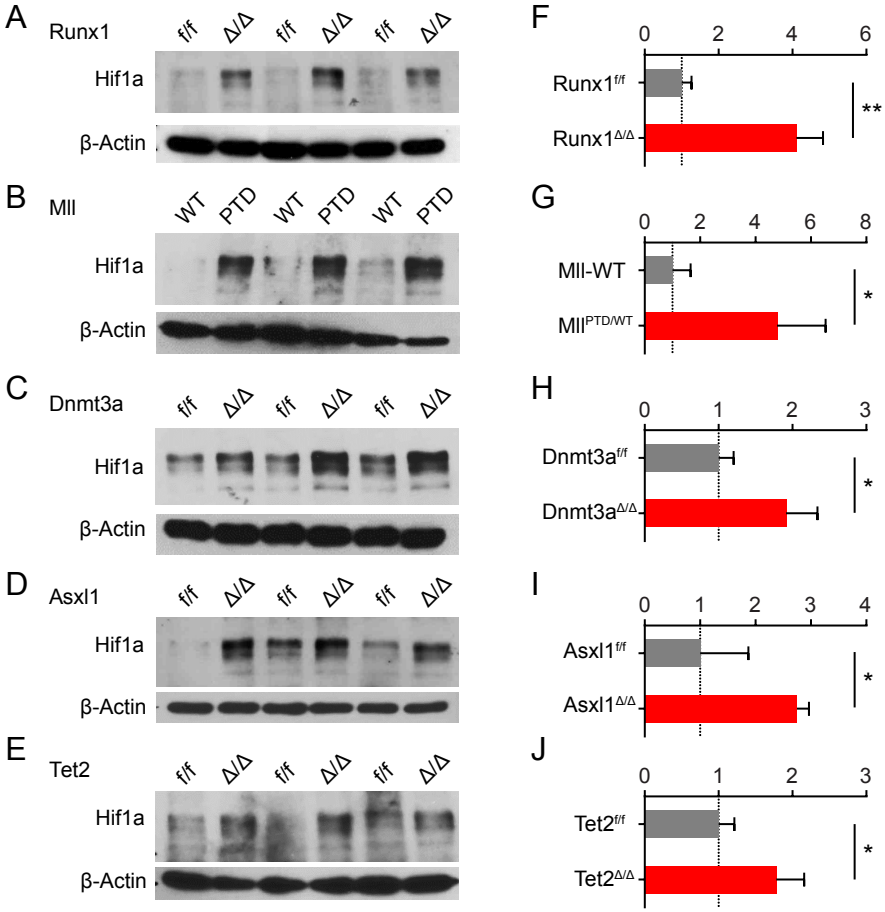

Figure S3. HIF1A Protein Accumulation Induced by MDS-associated Mutations. A-E, Hif1a protein expression in the c-Kit$^+$ cells from indicated mice. *Runx1*$^{f/f}$ and *Vav1*-Cre/*Runx1*$^{f/f}$ (*Runx1*$^{\Delta/\Delta}$), *Mll*-WT, and *Mll*$^{PTD/WT}$ mice without poly(I:C) injection were used in (S3A and S3B). *Dnmt3a*$^{f/f}$, *Mx1*-Cre/*Dnmt3a*$^{f/f}$, *Asxl1*$^{f/f}$, *Mx1*-Cre/*Asxl1*$^{f/f}$, *Tet2*$^{f/f}$, *Mx1*-Cre/*Tet2*$^{f/f}$ treated with poly(I:C) were used in (S3C-S3E). BM cells were harvested 2 to 3 weeks after final poly(I:C) injection. **F-J,** Quantification of Hif1a protein expression in the c-Kit$^+$ cells from indicated mice. Results were normalized to the expression level in c-Kit$^+$ cells from control mice for each. Data are mean ± s.d. *$P < 0.05$, **$P < 0.01$.

Figure S4 Hayashi. *et al*.

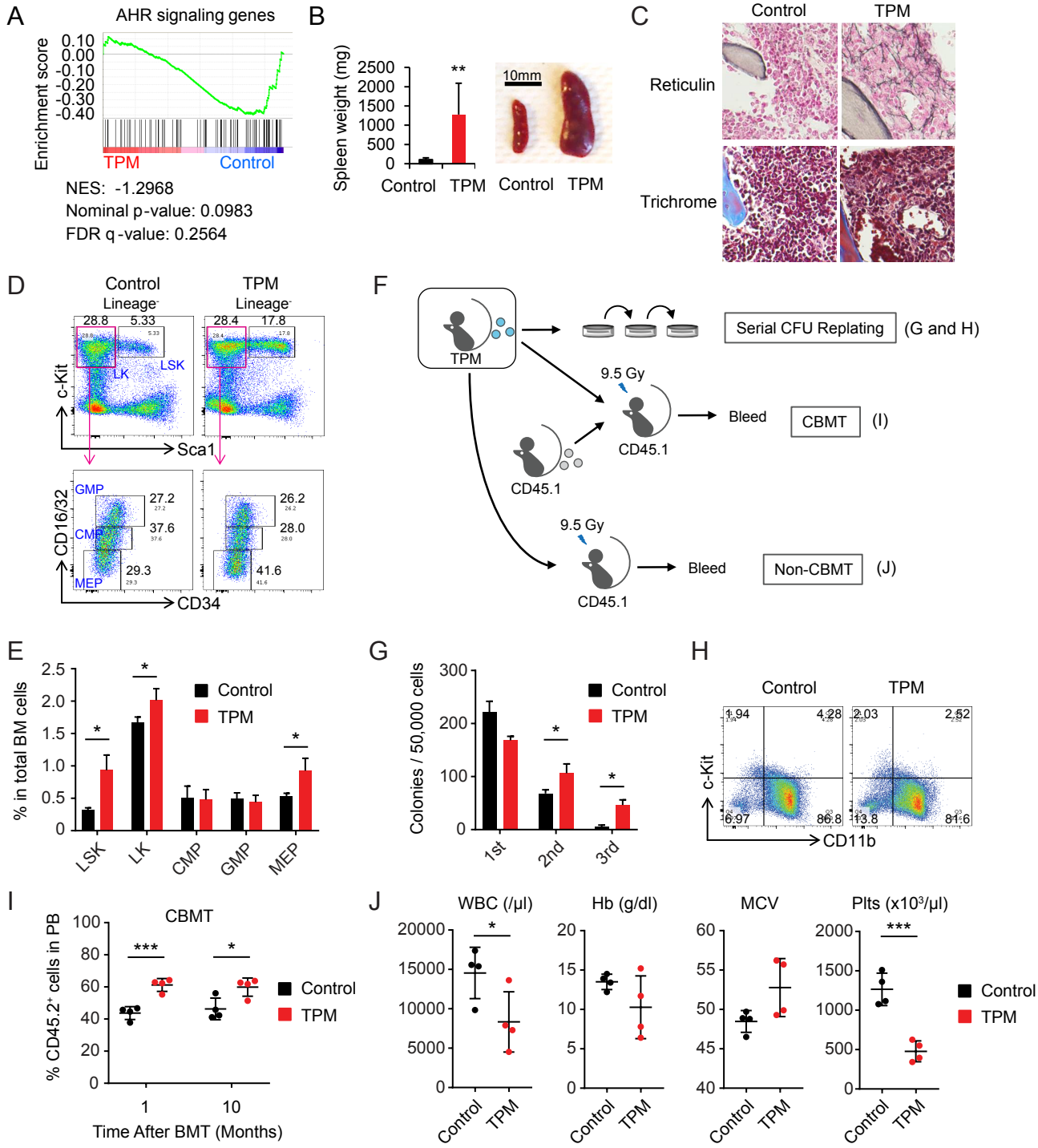

Figure S4. HIF1A Activates Immune Cells. A, GSEA plot showing decreased gene expression of AHR targets in c-Kit$^+$ BM cells from *Vav1*-Cre/TPM mice relative to *Vav1*-Cre/LSL-tTA mice (*Vav1*-Cre/Control). NES, *P* value, and FDR are shown. **B,** Splenomegaly observed in *Vav1*-Cre/TPM mice. **C,** Reticulin and trichrome staining of the BM from *Vav1*-Cre/Control and *Vav1*-Cre/TPM mice. Data are mean ± s.d. **D-E,** Flow cytometric analysis of 7AAD$^-$ lineage marker negative (lineage$^-$) single whole BM cells from *Vav1*-Cre/Control and *Vav1*-Cre/TPM mice (n = 3 per each group) (D). Percentage of cells in the lineage$^-$, c-Kit$^+$, Sca-1$^+$ cells (LSK), lineage$^-$, c-Kit$^+$, Sca-1$^-$ cells (LK), common myeloid progenitor (CMP) (LK, CD16/32$^-$, CD34$^+$), granulocyte/macrophage progenitor (GMP) (LK, CD16/32$^+$, CD34$^+$), and megakaryocyte/erythroid progenitor (MEP) (LK, CD16/32$^-$, CD34$^-$) in BM (*n* = 3 per each group) in BM is shown in (E). Data are mean ± s.d. **F,** Schematic of CFU replating assay, competitive BMT assay, and Non-competitive BMT assay. **G,** Serial CFU replating assay of BM cells from indicated genotypes. Doxycycline (1 μg/ml) was added in the M3434 methylcellulose medium. Data are mean ± s.d. from triplicate cultures. **H,** Flow cytometric analysis of cells forming primary colonies in (G). **I,** PB chimerism (as measured by CD45.2 marker) from 1:1 ratio competitive BMT assay from the primary *Vav1*-Cre/TPM mice showing MDS phenotypes and control mice. Equal number of BM cells from B6.SJL mice (CD45.1) as a competitor. Doxycycline administration was continued after the engraftment. **J,** Blood count after Non-competitive BMT assay from the primary *Vav1*-Cre/TPM mice showing MDS phenotypes and control mice. WBC, HB, MCV, and Plts counts in PB from the recipient mice are shown. Data are mean ± s.d. **P* < 0.05, ***P* < 0.01, ****P* < 0.001; NS, not significant.

Figure S5 Hayashi. *et al*.

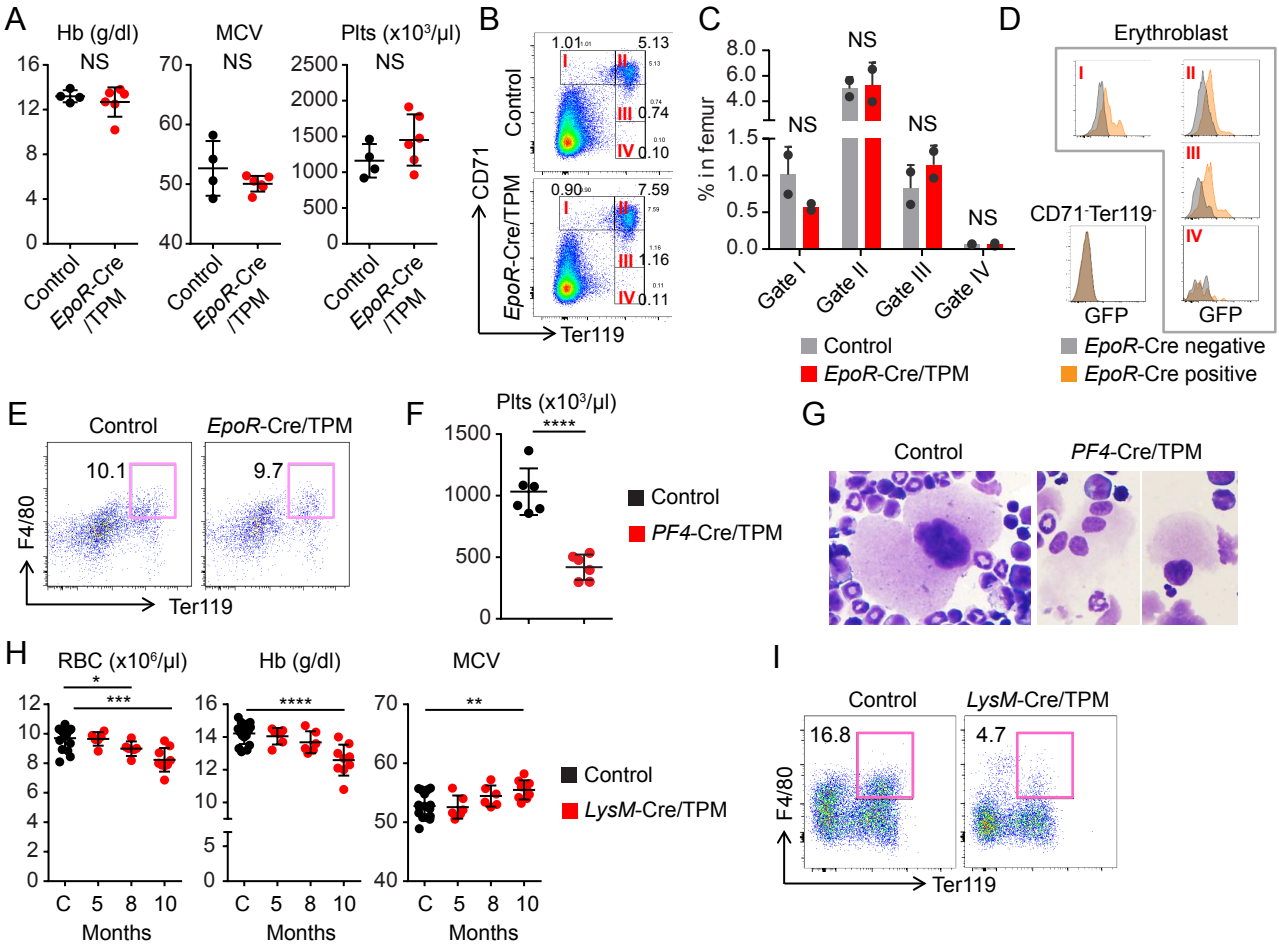

Figure S5. HIF1A induction in the erythroid, megakaryocyte, and myelomonocytic lineages A, HB, MCV, and Plts counts in PB from *EpoR*-Cre/*LSL*-rtTA (*EpoR*-Cre/Control) mice ($n = 4$) and *EpoR*-Cre/*LSL*-rtTA/TPM (*EpoR*-Cre/TPM) mice ($n = 6$). Data are mean ± s.d. **B,** Flow cytometric analysis of $7AAD^-$ single whole BM cells from *EpoR*-Cre/Control and *EpoR*-Cre/TPM mice. **C,** Percentages of proerythroblasts (gate I), basophilic erythroblasts (gate II), polychromatic erythroblast (gate III), and orthochromatic erythroblasts (gate IV) in femur from *EpoR*-Cre/Control and *EpoR*-Cre/TPM mice ($n = 2$ per each group). Data are mean ± s.d. **D,** GFP expression in the each erythroblast population in (B) and $CD71^-$ $Ter119^-$ non-erythroid population. Representative data is shown. *EpoR*-Cre -negative mouse was used as a GFP-negative control. **E,** Flow cytometric analysis of $7AAD^-$ $Gr\text{-}1^-$ 115^- multiplets from *EpoR*-Cre/Control and *EpoR*-Cre/TPM mice. **F,** Plts counts in PB from *PF4*-Cre/*LSL*-rtTA (*PF4*-Cre/Control) mice and *PF4*-Cre/*LSL*-rtTA/TPM (*PF4*-Cre/TPM) mice ($n = 6$ per each group). Data are mean ± s.d. **G,** Wright Giemsa staining of BM cells from *PF4*-Cre/Control and *PF4*-Cre/TPM mice. **H,** RBC counts, HB, and MCV in PB from *LysM*-Cre/Control mice ($n = 16$, 5 months to 10 months after HIF1A induction) and *LysM*-Cre/TPM mice ($n = 6$, 5 months after HIF1A induction; $n = 6$, 8 months after HIF1A induction; $n = 9$, 10 months after HIF1A induction). Data are mean ± s.d. **I,** Flow cytometric analysis of $7AAD^-$ $Gr\text{-}1^-$ 115^- multiplets from *LysM*-Cre/*LSL*-rtTA (*LysM*-Cre/Control) mice and *LysM*-Cre/*LSL*-rtTA/TPM (*LysM*-Cre/TPM) mice. $*P < 0.05$, $**P < 0.01$, $***P < 0.001$, $****P < 0.0001$; NS, not significant.

Figure S6 Hayashi. *et al*.

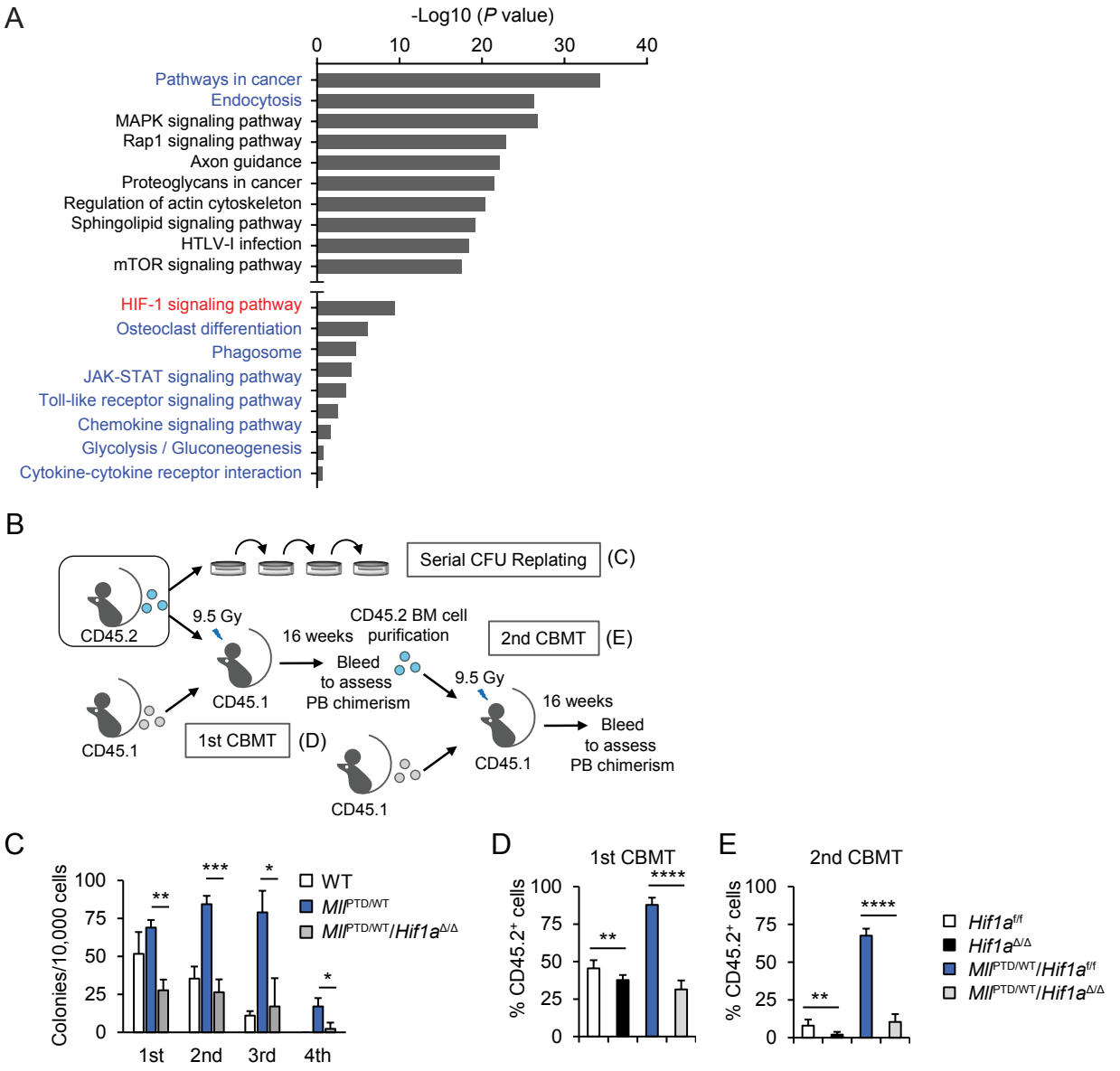

Figure S6. Critical role of activated HIF1A signaling in MLL-PTD-mediated Clonal Advantage. **A,** Cross comparison of the H3K4me3 ChIP-Seq data with the ENCODE binding data of $CD34^+$ myeloid progenitors (control_ENCFF565KJC.bam, H3K4me3_ENCFF218HFN.bam; https://www.encodeproject.org/experiments/ENCSR072ENL/). KEGG pathway enrichment analysis on genes of the overlapped binding sites. False discovery rate (FDR) < 0.001 was used. **B,** Schematic of CFU replating assay and serial competitive BMT assay. **C,** Serial CFU replating assay of BM cells from indicated genotypes. Data are mean ± s.d. from triplicate cultures. **D-E,** PB chimerism (as measured by CD45.2 marker) from 2 consecutive serial competitive BMT assay from the indicated genotypes (n = 8 to15 per group). Data are mean ± s.d. *P < 0.05, **P < 0.01, ***P < 0.001, ****P < 0.0001.

Figure S7 Hayashi. *et al*.

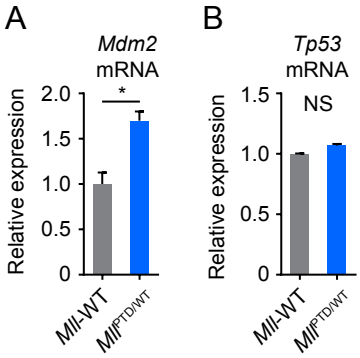

Figure S7. Metabolic shift in *Mll*$^{PTD/WT}$ mice. A-B, *Mdm2* mRNA and *Tp53* mRNA expression in the c-Kit^{+} cells from indicated mice. Data are mean ± s.d. **P* < 0.05, ***P* < 0.01; NS, not significant.

Figure S8 Hayashi. *et al*.

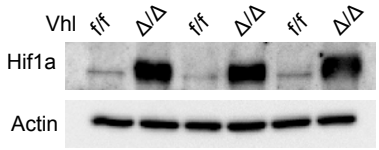

Figure S8. HIF1A protein is constantly degraded by PHD-VHL axis in BM. Hif1a protein expression in the purified c-Kit^{+} cells from indicated mice.

Figure S9 Hayashi. *et al*.

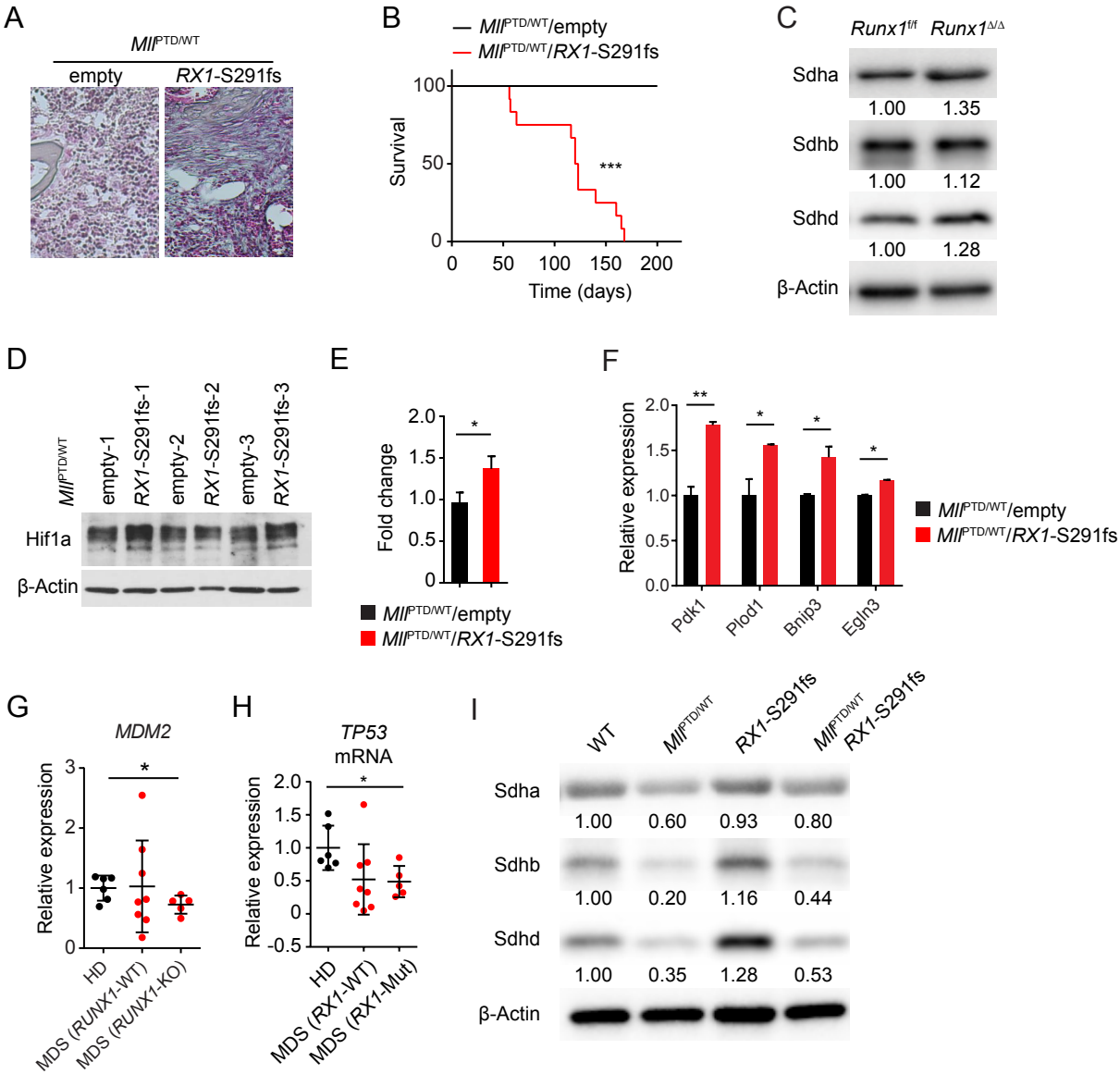

Figure S9. Phenotype of *Mll*$^{PTD/WT}$/*Rx1-S291fs* mice. A, Reticulin staining of BM from *Mll*$^{PTD/WT}$/empty and *Mll*$^{PTD/WT}$/*Rx1-S291fs* mice. **B,** Survival of *Mll*$^{PTD/WT}$/empty ($n = 8$) and *Mll*$^{PTD/WT}$/*Rx1*-S291fs ($n = 12$) BMT mice. **C,** Sdha, Sdhb, and Sdhd protein expression in the c-Kit$^+$ cells from indicated mice. **D,** Hif1a protein expression in the cells from primary colonies. **E,** Quantification of Hif1a protein expression in (C). Results were normalized to the expression level in the control cells. Data are mean ± s.d. **F,** Known Hif1a target gene expression in the c-Kit$^+$ cells from indicated mice. Data are mean ± s.d. **G-H,** *MDM2* mRNA and *TP53* mRNA expression in BM mononuclear cells from healthy donors ($n = 6$) and MDS patients (*RUNX1*-wild type, $n = 8$; *RUNX1*-mutation, $n = 5$). **I,** Sdha, Sdhb, and Sdhd protein expression in the c-Kit$^+$ cells from indicated mice. *$P < 0.05$, **$P < 0.01$, ***$P < 0.001$.

Figure S10 Hayashi. *et al*.

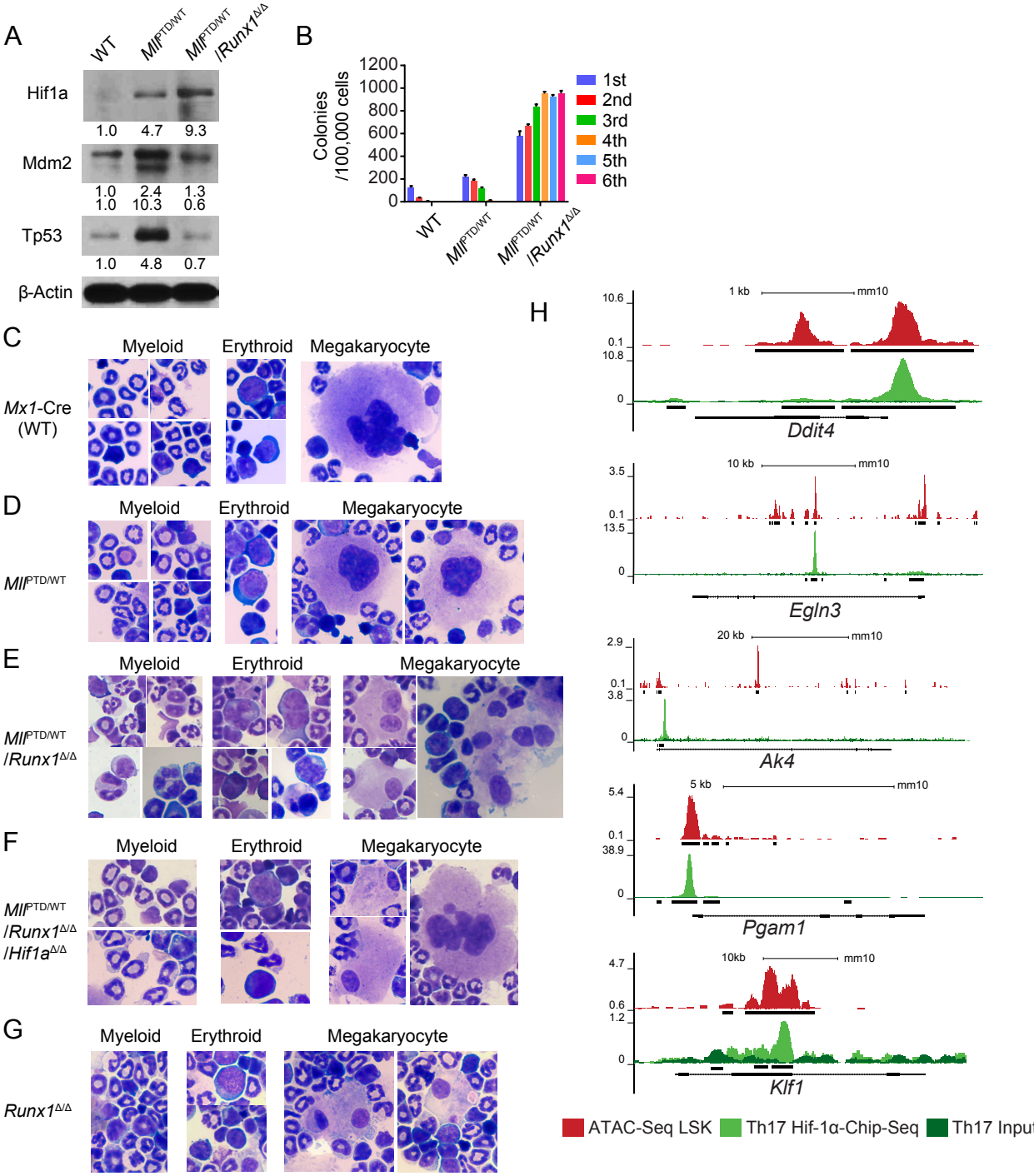

Figure S10. Genetic Deletion of *Runx1* in *Mll*$^{PTD/WT}$ mice. A, Hif1a, Mdm2, and Tp53 protein expression in the c-Kit^{+} cells from indicated mice. **B,** Serial CFU replating assay of BM cells from indicated genotypes. Data are mean ± s.d. from triplicate cultures. **C-G,** BM morphology of indicated mice. **H,** ATAC-Seq and HIF1A ChIP-Seq tracks illustrating co-regulation at select loci of representative genes shown in Figure 6F. The data of ATAC–Seq analysis, which indicates the location of open-chromatin, in LSK cells (GSM1463179) and HIF1A ChIP-Seq (GSE40918) analysis were obtained from GEO record.

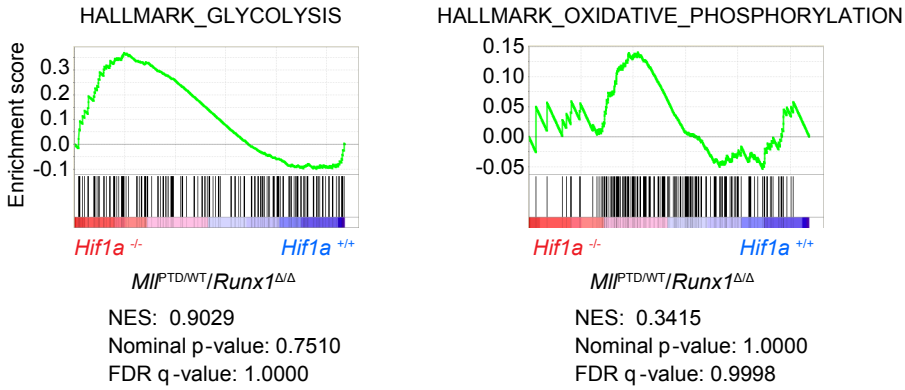

Figure S11. Pseudohypoxia related signature after Hif1a deletion. GSEA plots showing genes related to glycolysis and mitochondrial oxidative phosphorylation in c-Kit^{+} BM cells from *Mll*$^{PTD/WT}$/*Runx1*$^{\Delta/\Delta}$ cells with or without Hif1a deletion. NES, *P* value, and FDR are shown.

Figure S12 Hayashi. *et al*.

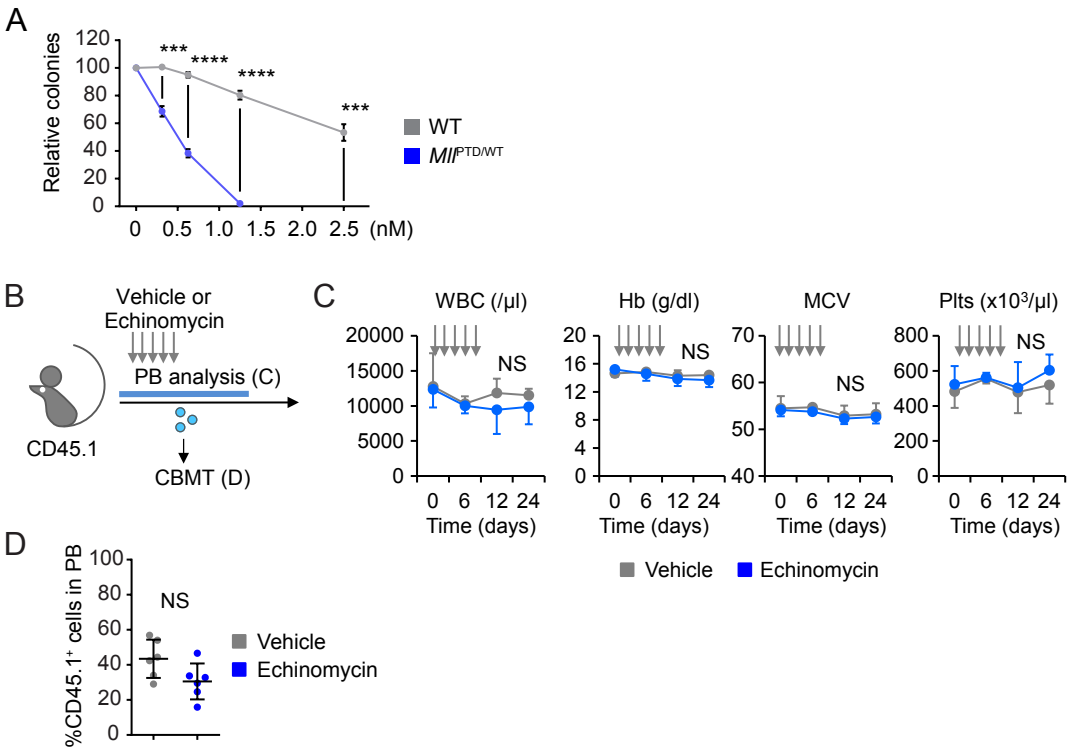

Figure S12. Effect of Echinomycin on normal hematopoiesis. A, Echinomycin treatment in CFU assay using WT and *Mll*$^{PTD/WT}$ BM cells. Colony numbers were normalized to those in the control. Data are mean ± s.d. from independent 3 experiments. **B,** Schematic of drug treatment, analysis, and competitive BMT assays in (C and D). **C,** WBC, HB, MCV, and Plts counts in PB from vehicle treated control mice and Echinomycin treated mice (n = 4 to 6 per each group). Data are mean ± s.d. **D,** PB chimerism (as measured by CD45.1 marker) at 4 months after CBMT (n = 5 per each group). Data are mean ± s.d., ***P < 0.001, ****P < 0.0001; NS, not significant.

Figure S13 Hayashi. *et al*.

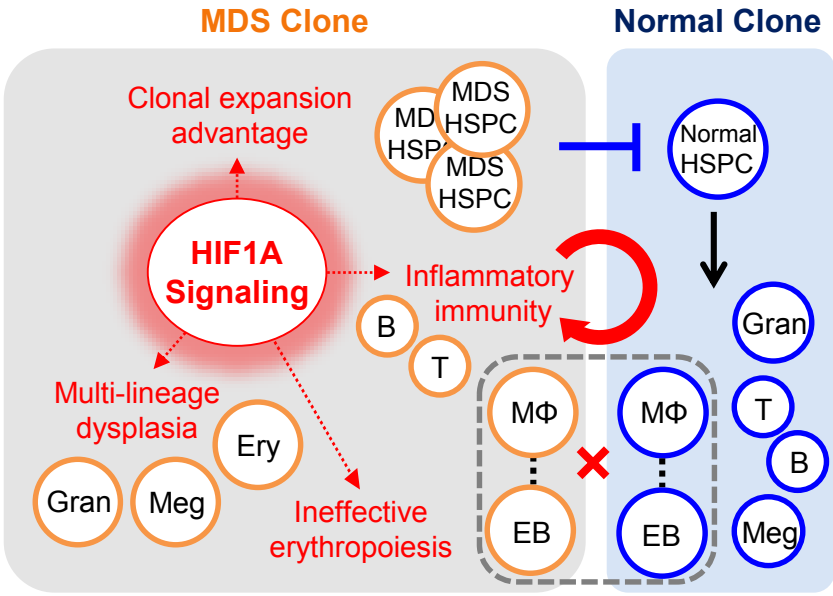

Figure S13. MDS Genesis through activated HIF1A signaling. Model for HIF1A signaling mediated MDS development. (1) MDS associated mutations activate HIF1A signaling in both MDS HSPCs and multi-lineages mature cells. (2) Activated HIF1A signaling gives clonal expansion advantage to MDS HSPCs. (3) Activated HIF1A signaling also causes dysplasia, activated inflammatory immunity, and ineffective erythropoiesis.

Table S1 **Up-regulated pathways in *Mll*$^{PTD/WT}$ mice**

Pathway	Genes
Systemic lupus erythematosus	C1ra C2 C3 C4b C6 C8g Cd28 Cd80 Cd86 Elane Fcgr1 Fcgr2b Fcgr3 Fcgr4 Gm12657 Gm14474 Gm14475 Gm14476 Gm14477 Gm14478 Gm14479 Gm14482 Gm14483 Gm14484 Gm14501 Gm16501 Gm4906 Gm5132 Gm6026 Grin2b H2-Aa H2-DMa H2-DMb1 H2-DMb2 H2-Eb1 H2-Oa H2-Ob H2afj H2afv H2afx H2afy H2afy2 H2afz H2bfm H3f3a H3f3b Hist1h2ab Hist1h2ac Hist1h2ad Hist1h2ae Hist1h2af Hist1h2ag Hist1h2ah Hist1h2ai Hist1h2ak Hist1h2an Hist1h2ao Hist1h2ap Hist1h2bb Hist1h2bc Hist1h2be Hist1h2bf Hist1h2bg Hist1h2bh Hist1h2bj Hist1h2bk Hist1h2bl Hist1h2bm Hist1h2bn Hist1h2bp Hist1h2bq Hist1h2br Hist1h3a Hist1h3b Hist1h3c Hist1h3d Hist1h3e Hist1h3f Hist1h3g Hist1h3h Hist1h3i Hist1h4a Hist1h4b Hist1h4c Hist1h4d Hist1h4f Hist1h4h Hist1h4i Hist1h4j Hist1h4k Hist1h4m Hist1h4n Hist2h2aa1 Hist2h2aa2 Hist2h2ab Hist2h2ac Hist2h2bb Hist2h2be Hist2h3b Hist2h3c1 Hist2h3c2 Hist2h4 Hist4h4 Ifng Snrpd3 Tnf Trim21
Phagosome	Actb Actg1 Atp6ap1 Atp6v0a1 Atp6v0a2 Atp6v0b Atp6v0c Atp6v0d1 Atp6v1a Atp6v1c1 Atp6v1e1 Atp6v1e2 Atp6v1g1 Atp6v1g2 C1ra C3 Calr Cd14 Cd209a Cd209b Cd209c Cd209f Clec7a Colec12 Coro1a Ctss Cyba Cybb Dync1i2 Dync1li1 Dync1li2 Fcgr1 Fcgr2b Fcgr3 Fcgr4 H2-Aa H2-Bl H2-D1 H2-DMa H2-DMb1 H2-DMb2 H2-Eb1 H2-K1 H2- M10.1 H2-M10.2 H2-M10.4 H2-M3 H2-M9 H2-Oa H2-Ob H2-Q1 H2-Q10 H2-Q2 H2-Q6 H2-Q7 H2-Q8 H2-T10 H2-T22 H2-T23 H2-T24 H2-T3 H2-T9 Itga5 Itgam Itgav Itgb2 Itgb2l Itgb5 LOC547349 M6pr Mbl1 Mpo Ncf1 Ncf2 Ncf4 Nos1 Olr1 Pla2r1 Rab5b Rab5c Rab7 Rac1 Rilp Scarb1 Sec61a1 Sec61a2 Sec61b Sec61g Sftpa1 Stx18 Stx7 Tap1 Tap2 Tcirg1 Tfrc Thbs3 Thbs4 Tlr2 Tlr4 Tlr6 Tuba1a Tuba1b Tuba1c Tuba3a Tuba4a Tuba8 Tubb1 Tubb2b Tubb3 Tubb5 Tubb6
Chemokine signaling pathway	Adcy1 Adcy4 Adcy6 Adcy7 Adrbk1 Akt1 Arrb2 Bcar1 Braf Ccl17 Ccl19 Ccl21a Ccl21c Ccl24 Ccl26 Ccl27a Ccl28 Ccl3 Ccl4 Ccl6 Ccl8 Ccl9 Ccr1 Ccr10 Ccr1l1 Ccr2 Ccr3 Ccr5 Ccr6 Ccr7 Ccr8 Ccr9 Cdc42 Chuk Crk Crkl Csk Cx3cr1 Cxcl1 Cxcl11 Cxcl13 Cxcl14 Cxcl15 Cxcl16 Cxcl2 Cxcl5 Cxcl9 Cxcr4 Cxcr5 Dock2 Elmo1 Fgr Foxo3 Gm13306 Gm5741 Gnai1 Gnai2 Gnai3 Gnb3 Gnb4 Gng10 Gng12 Gng2 Gng7 Gng8 Gngt2 Grb2 Grk1 Grk5 Grk6 Gsk3a Jak2 Jak3 Map2k1 Mapk1 Mapk3 Ncf1 Nfkbia Nfkbib Pf4 Pik3cd Pik3cg Pik3r1 Pik3r2 Plcb2 Plcb3 Prex1 Prkaca Prkcb Prkcd Prkx Ptk2b Pxn Rac1 Rac2 Rap1a Rap1b Rasgrp2 Rhoa Rock2 Shc1 Shc4 Stat1 Stat3 Stat5b Tiam1 Tiam2 Vav1 Wasl Xcl1
Cytokine-cytokine receptor interaction	Acvr2b Amh Amhr2 Ccl17 Ccl19 Ccl21a Ccl21c Ccl24 Ccl27a Ccl28 Ccl3 Ccl4 Ccl6 Ccl8 Ccl9 Ccr1 Ccr10 Ccr1l1 Ccr2 Ccr3 Ccr5 Ccr6 Ccr7 Ccr8 Ccr9 Cd27 Cd70 Clcf1 Cntfr Csf1 Csf1r Csf2 Csf2ra Csf2rb Csf2rb2 Csf3 Csf3r Cx3cr1 Cxcl1 Cxcl11 Cxcl13 Cxcl14 Cxcl15 Cxcl16 Cxcl2 Cxcl5 Cxcl9 Cxcr4 Cxcr5 Epor Flt3 Flt3l Ifna1 Ifna11 Ifna12 Ifna13 Ifna14 Ifna2 Ifna4 Ifna5 Ifna6 Ifna7 Ifna9 Ifnab Ifnar2 Ifnb1 Ifne Ifng Ifngr1 Ifngr2 Il11ra1 Il11ra2 Il12a Il12b Il12rb1 Il15ra Il17ra Il17rb Il18 Il18r1 Il18rap Il1a Il1b Il1r1 Il1r2 Il2 Il20 Il20ra Il22 Il22ra1 Il23a Il3 Il3ra Il4ra Il5 Il6 Il6ra Inhba Inhbc Inhbe Kit Lif Lta Ltb Mpl Osm Pdgfb Pf4 Relt Tgfb1 Tgfb3 Tgfbr2 Tnf Tnfrsf10b Tnfrsf11a Tnfrsf12a Tnfrsf13b Tnfrsf14 Tnfrsf18 Tnfrsf1a Tnfrsf1b Tnfrsf21 Tnfrsf4 Tnfrsf9 Tnfsf10 Tnfsf12 Tnfsf13 Tnfsf14 Tnfsf8 Vegfa Xcl1
Endocytosis	Acap1 Acap2 Acap3 Adrb2 Adrbk1 Agap2 Ap2s1 Arap1 Arap2 Arap3 Arf6 Arfgap1 Arfgap2 Arrb2 Asap1 Cav1 Cav2 Cav3 Cbl Cblc Ccr5 Cdc42 Chmp1a Chmp2a Chmp4b Chmp6 Csf1r Cxcr4 Dnajc6 Dnm2 Ehd1 Epn2 Eps15 Erbb3 Fgfr4 Git2 Grk1 Grk5 Grk6 H2-Bl H2-D1 H2-K1 H2-M10.1 H2-M10.2 H2-M10.4 H2-M3 H2-M9 H2-Q1 H2-Q10 H2-Q2 H2-Q6 H2-Q7 H2-Q8 H2-T10 H2-T22 H2-T23 H2-T24 H2-T3 H2-T9 Hspa8 Iqsec1 Itch Kit Ldlr Ldlrap1 LOC547349 Mdm2 Nedd4 Nedd4l Pard6a Pard6g Pdcd6ip Pip5k1b Pip5k1c Pip5k1l Pld1 Pml Psd Psd2 Psd3 Psd4 Rab11a Rab11b Rab11fip3 Rab11fip4 Rab31 Rab5b Rab5c Rab7 Ret Rhoa Rnf41 Rufy1 Sh3gl2 Sh3glb1 Smad2 Smad3 Smad7 Snf8 Stam Stambp Tfrc Tgfb1 Tgfb3 Tgfbr2 Vps28 Vps36 Vps37b Vps45 Vps4a Vps4b Zfyve20 Zfyve9
Toll-like receptor signaling pathway	Akt1 Casp8 Ccl3 Ccl4 Cd14 Cd80 Cd86 Chuk Cxcl11 Cxcl9 Fos Ifna1 Ifna11 Ifna12 Ifna13 Ifna14 Ifna2 Ifna4 Ifna5 Ifna6 Ifna7 Ifna9 Ifnab Ifnar2 Ifnb1 Ikbke Il12a Il12b Il1b Il6 Irf7 Lbp Ly96 Map2k1 Map2k2 Map2k3 Map2k4 Map2k6 Map2k7 Map3k7 Mapk1 Mapk11 Mapk12 Mapk13 Mapk14 Mapk3 Mapk9 Myd88 Nfkbia Pik3cd Pik3cg

	Pik3r1 Pik3r2 Rac1 Spp1 Stat1 Tbk1 Ticam1 Ticam2 Tirap Tlr1 Tlr2 Tlr3 Tlr4 Tlr6 Tlr9 Tnf Tollip Traf3
Osteoclast differentiation	Akt1 Blnk Btk Camk4 Chuk Csf1 Csf1r Cyba Cybb Fcgr1 Fcgr2b Fcgr3 Fcgr4 Fos Fosb Fosl2 Gab2 Grb2 Ifnar2 Ifnb1 Ifng Ifngr1 Ifngr2 Il1a Il1b Il1r1 Irf9 Junb Jund Lcp2 Lilra6 Map2k1 Map2k6 Map2k7 Map3k14 Map3k7 Mapk1 Mapk11 Mapk12 Mapk13 Mapk14 Mapk3 Mapk9 Mitf Ncf1 Ncf2 Ncf4 Nfatc1 Nfkb2 Nfkbia Oscar Pik3cd Pik3cg Pik3r1 Pik3r2 Pira1 Pira4 Pira6 Ppp3ca Rac1 Relb Sirpa Socs3 Sqstm1 Stat1 Syk Tec Tgfb1 Tgfbr2 Tnf Tnfrsf11a Tnfrsf1a Trem2 Tyk2 Tyrobp
Pathways in cancer	Abl1 Akt1 Apc Apc2 Ar Arnt Axin1 Bad Bax Bcl2l1 Bcr Bid Birc3 Braf Casp8 Casp9 Cbl Cblc Ccdc6 Cdc42 Cdk2 Cdk4 Cdk6 Cdkn1a Cdkn2a Chuk Cks1b Crk Crkl Csf1r Csf2ra Csf3r Ctnna1 Ctnna3 Ctnnb1 Cycs Cyct Dapk3 Dvl1 Dvl2 E2f2 Egln1 Egln2 Egln3 Ep300 Erbb2 Fgf1 Fgf12 Fgf14 Fgf17 Fgf2 Fgf22 Fgf3 Fgf7 Fgf9 Flt3 Flt3l Fos Fzd3 Fzd5 Fzd8 Fzd9 Gli1 Grb2 Hsp90aa1 Hsp90ab1 Il6 Itga2b Itga6 Itgav Kit Lama3 Lamb2 Map2k1 Map2k2 Mapk1 Mapk3 Mapk9 Mdm2 Mecom Mitf Mlh1 Mmp1b Msh2 Msh3 Msh6 Ncoa4 Nfkb2 Nfkbia Nos2 Pdgfb Pgf Pias1 Pias2 Pias4 Pik3cd Pik3cg Pik3r1 Pik3r2 Pml Ppard Prkcb Rac1 Rac2 Rala Ralgds Rara Rarb Rassf5 Ret Rhoa Runx1 Rxrb Slc2a1 Smad2 Smad3 Smad4 Stat1 Stat3 Stat5b Stk36 Stk4 Tceb2 Tgfb1 Tgfb3 Tgfbr2 Tpm3 Traf1 Traf3 Traf4 Traf5 Vegfa Wnt1 Wnt10b Wnt16 Wnt2b Wnt3 Wnt4 Wnt5b Wnt7a Wnt9b
Jak-STAT signaling pathway	Akt1 Bcl2l1 Cbl Cblc Ccnd3 Cish Clcf1 Cntfr Csf2 Csf2ra Csf2rb Csf2rb2 Csf3 Csf3r Ep300 Epor Gh Grb2 Ifna1 Ifna11 Ifna12 Ifna13 Ifna14 Ifna2 Ifna4 Ifna5 Ifna6 Ifna7 Ifna9 Ifnab Ifnar2 Ifnb1 Ifne Ifng Ifngr1 Ifngr2 Il11ra1 Il11ra2 Il12a Il12b Il12rb1 Il15ra Il2 Il20 Il20ra Il22 Il22ra1 Il23a Il3 Il3ra Il4ra Il5 Il6 Il6ra Irf9 Jak2 Jak3 Lif Mpl Osm Pias1 Pias2 Pias4 Pik3cd Pik3cg Pik3r1 Pik3r2 Pim1 Ptpn11 Ptpn6 Socs3 Socs5 Spry3 Stam Stat1 Stat3 Stat5b Stat6 Tyk2
Glycolysis / Gluconeogenesis	Acss1 Adh4 Adh5 Adh7 Adpgk Aldh1b1 Aldh2 Aldh3a2 Aldh3b1 Aldh9a1 Aldoa Aldob Bpgm Dld Eno1 Eno2 Eno3 Fbp1 Fbp2 G6pc Galm Gapdh Gapdhs Gck Gpi1 Hk1 Hk2 Hk3 Ldha Ldhb Ldhc Pck1 Pfkl Pgam1 Pgam2 Pklr Pkm Tpi1

Table S3. Sequence information for primers

Gene	Forward primer sequence (5'-3')	Reverse primer sequence (5'-3')
MDM2	GAAGGAAACTGGGGAGTCTTG	GGTCTCTTGTTCCGAAGCTG
TP53	GTACATCTGGCCTTG AAACC	AGCTGCCCAACTGTAGAAAC
HIF1A	AGGTGGATATGTCTGGGTTG	AAGGACACATTCTGTTTGTTG
ACTB	CACCCAGCACAATGAAGATC	GTCATAGTCCGCCTAGAAGC

Gene	Forward primer sequence (5'-3')	Reverse primer sequence (5'-3')
Mdm2	TCCGAGCCTGGGTCTGTGTG	ATGCGAGGGCGTCTCTGTGG
Tp53	ACGCTTCTCCGAAGACTGG	AGGGAGCTCGAGGCTGATA
Hprt1	CAGTCCCAGCGTCGTGATTA	GGCCTCCCATCTCCTTCATG
Actb	GCTCTTTTCCAGCCTTCCTT	CTTCTGCATCCTGTCAGCAA
Plod1	GAACTGAGCTGAACGCTTGA	AAGGATGACGCCAAGCTAGA
Egln3	CTGGATAGCAAGCCACCATT	CATCAACTTCCTCCTGTCCC
Bnip3	TGAAGTGCAGTTCTACCCAGG	CCTGTCGCAGTTGGGTTC
Pdk1	TTACTCAGTGGAACACCGCC	GTTTATCCCCCGATTCAGGT
Idh1	TATGATGGGCGTTTCAAAGA	TGAGCCTGTGTTCATAGCAGA
Idh2	GGATGTACAACACCGACGAGT	CGGCCATTTCTTCTGGATAG
Idh3a	CAGGTGACAAGAGGTTTTGC	TGAAATTTCTGGGCCAATTC
Idh3b	GCTGCGGCATCTCAATCT	CCATGTCTCGAGTCCGTACC
Idh3g	TCTCCTCTGCCGTCCTTG	ACTGAGGAAATGCTCCTTCG
Sdha	AGCCGTTTGGGGAACACTGG	TAGCAGGAGGTACGGTGGCA
Sdhb	ACGAGTGCATCCTGTGTGCC	TGCATGAGAACTGCAGGCCC
Sdhc	ACTGTCCGTTTGCCACCGAG	TTGGCCCCAAACACAGGGAC
Sdhd	TCTTGGGGCTGATCCCTGCT	ACCACTTGTCCAAGGCCCCA
Sdhaf1	GACATGCTGTGATACACCAACC	CGATGGGAGGAGAAAGTGC
Sdhaf2	CGGTGGTCACCTTGATCC	CGTCTGAATGATGTCACACTAGG
Sdhaf3	TCTTGAAGGAATGGGAGACG	TTTTCCAGTTGAGCTTTGTCTG
Sdhaf4	CCGTTTCACGGATGACTTTC	TTCCTCAAAGAATGATTCAGAAGA
Fh1	GCACCCCAATGATCATGTTA	ATTGCTGTGGGAAAGGTGTC

REFERENCES

1. Semenza GL. Targeting HIF-1 for cancer therapy. Nat Rev Cancer **2003**;3(10):721-32 doi 10.1038/nrc1187.